

## DNA-Decorated Two-Dimensional Crystalline Nanosheets

Shine K. Albert, Irla Sivakumar, Murali Golla, Hari Veera Prasad Thelu,  
Nithiyanandan Krishnan, Joseph Libin K. L., \* Ashish, and Reji Varghese

*J. Am. Chem. Soc.*, **Just Accepted Manuscript** • DOI: 10.1021/jacs.7b09283 • Publication Date (Web): 13 Nov 2017

Downloaded from <http://pubs.acs.org> on November 13, 2017

### Just Accepted

“Just Accepted” manuscripts have been peer-reviewed and accepted for publication. They are posted online prior to technical editing, formatting for publication and author proofing. The American Chemical Society provides “Just Accepted” as a free service to the research community to expedite the dissemination of scientific material as soon as possible after acceptance. “Just Accepted” manuscripts appear in full in PDF format accompanied by an HTML abstract. “Just Accepted” manuscripts have been fully peer reviewed, but should not be considered the official version of record. They are accessible to all readers and citable by the Digital Object Identifier (DOI®). “Just Accepted” is an optional service offered to authors. Therefore, the “Just Accepted” Web site may not include all articles that will be published in the journal. After a manuscript is technically edited and formatted, it will be removed from the “Just Accepted” Web site and published as an ASAP article. Note that technical editing may introduce minor changes to the manuscript text and/or graphics which could affect content, and all legal disclaimers and ethical guidelines that apply to the journal pertain. ACS cannot be held responsible for errors or consequences arising from the use of information contained in these “Just Accepted” manuscripts.

## DNA-Decorated Two-Dimensional Crystalline Nanosheets

Shine K. Albert,<sup>†</sup> Irla Sivakumar,<sup>†</sup> Murali Golla,<sup>†</sup> Hari Veera Prasad Thelu,<sup>†</sup> Nithiyanandan Krishnan,<sup>†</sup> Joseph Libin K. L.,<sup>†</sup> Ashish,<sup>‡</sup> Reji Varghese\*<sup>†</sup>

<sup>†</sup>School of Chemistry, Indian Institute of Science Education and Research (IISER) Thiruvananthapuram, Trivandrum-695551, Kerala, India

<sup>‡</sup>Protein Science and Engineering Division, Institute of Microbial Technology, Sector 39-A, Chandigarh-160036, India

*Supporting Information Placeholder*

**ABSTRACT:** Design and synthesis of high aspect ratio 2D nanosheets with surface having ultra-dense array of information-rich molecule such as DNA is extremely challenging. Herein, we report a universal strategy based on amphiphilicity-driven self-assembly for the crafting of high aspect ratio, 2D sheets that are densely surface-decorated with DNA. Microscopy and X-ray analyses have shown that the sheets are crystalline. The most unique feature of the sheets is DNA-directed surface addressability, which is demonstrated through the decoration of either faces of the sheet with gold nanoparticles through sequence-specific DNA hybridization. Our results suggest that this design strategy can be applied as a general approach for the synthesis of DNA decorated high aspect ratio sheets, which may find potential applications in material science, drug delivery, and nanoelectronics.

Crafting of two-dimensional (2D) nanosheets with high aspect ratio is extremely important due to their potential applications in material science and nanotechnology.<sup>1</sup>

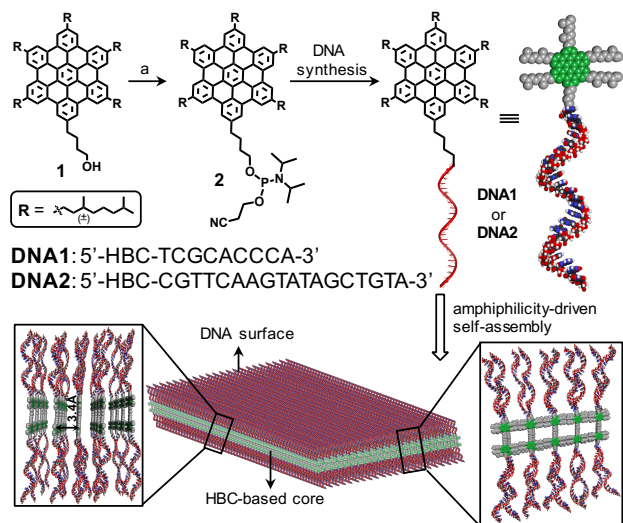
Even more beneficial would be the design of high aspect ratio sheets with surface having ultra-dense array of highly information-rich molecule like DNA. This is because DNA-directed surface addressability of such sheets makes it an ideal 2D nanoplatform for the precise organization of other functional molecules on their surface through sequence-specific DNA hybridization.<sup>2</sup> DNA nanotechnology has proven to be an ideal approach towards this goal as this strategy allows the self-assembly of DNAs into well-defined 2D and 3D nanostructures decorated with DNA.<sup>3</sup> Though the designing principles of DNA nanotechnology permit the fabrication of 2D sheets, the integration of other functional domains of interest into these systems is challenging. Hence, the development of a simple and general strategy for the synthesis of functional 2D nanosheets densely decorated with DNA is extremely important.

Self-assembly of DNA-amphiphiles, which combines the structural characteristics of DNA and the functional

properties of hydrophobic domain, offers a unique opportunity for the crafting of functional 2D and 3D nanomaterials with surface having ultra-dense array of DNA.<sup>4</sup> Recently, we have reported a series of DNA-amphiphiles and have shown their amphiphilicity-driven self-assembly into nano-to-micro sized DNAsomes.<sup>5</sup> We envisioned that the replacement of hydrophobic segment of DNAsome forming amphiphile with a strongly  $\pi$ -stacking hydrophobic core such as hexa-*peri*-benzocoronene (HBC) could direct the self-assembly into DNA decorated 2D sheets. Pioneering works of Aida et al.<sup>6</sup> and Müllen et al.<sup>7</sup> on the self-assembly of amphiphilic HBCs have shown the high propensity of HBC to assemble through  $\pi$ -stacking. However, DNA based amphiphilic systems of HBC have not yet been explored.

Herein we describe a simple, efficient, and general strategy based on amphiphilicity-driven self-assembly of DNA-amphiphile for the crafting of micrometer-sized, crystalline, 2D sheets that are densely surface-decorated with DNA. Sheet structure consists of DNA-based hydrophilic surface and a functional core that results from the self-assembly of alkylated HBC segment through  $\pi$ -stacking and van der Waals interactions. The unique feature of the nanosheet is the dense surface display of DNA, which allows the reversible decoration of the sheet surface with other functional molecules through sequence specific DNA hybridization. As a representative example, DNA-directed surface addressability of sheet is explored for the organization of Au-NPs on the surfaces of the sheet.

The covalent conjugation of alkyl chains ( $-C_{10}H_{21}$ ) tethered HBC segment to the hydrophilic DNA was achieved using the standard phosphoramidite chemistry (Scheme 1). The precursor alcohol **1** was synthesized following a reported procedure (SI).<sup>8</sup> The only structural difference between **DNA1** and **DNA2** is the length of the hydrophilic DNA segment, which is increased from **DNA1** (9-mer) to **DNA2** (18-mer) keeping the hydrophobic HBC core same (Scheme 1). Self-assembly of the amphiphile was achieved by annealing **DNA1/2**



18  
19  
20  
21  
22  
23

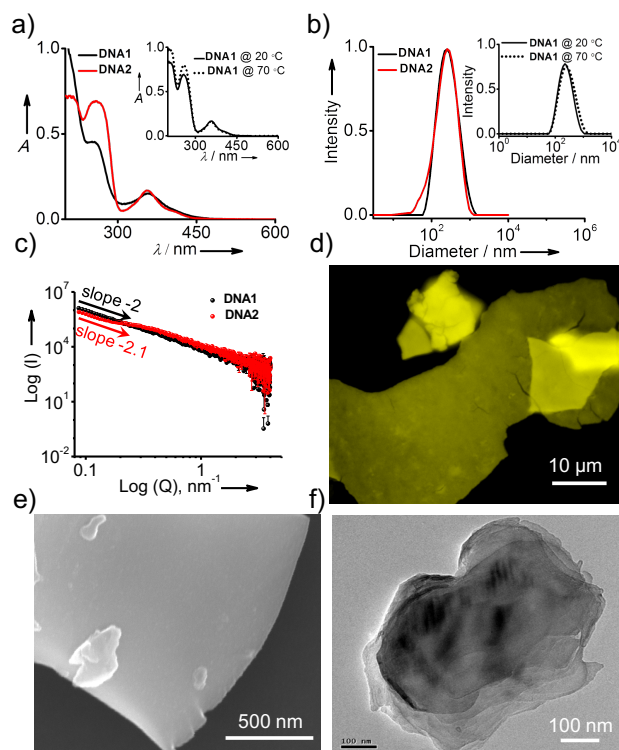
**Scheme 1.** Synthesis of **DNA1** and **DNA2**: a) dichloromethane, diisopropylamine, 2-cyanoethyl *N,N*-diisopropylchlorophosphoramidite, rt, 2h, 80%. Schematic representation depicting the amphiphilicity-driven self-assembly of **DNA1/2** into DNA-decorated 2D sheets. The protruding ssDNA on the sheet surface need not be rigid as shown.

24  
25

(1  $\mu$ M Tris-buffer, pH 7.3 or Milli-Q water) at 90  $^{\circ}$ C for 5 minutes followed by cooling to room temperature (rt).

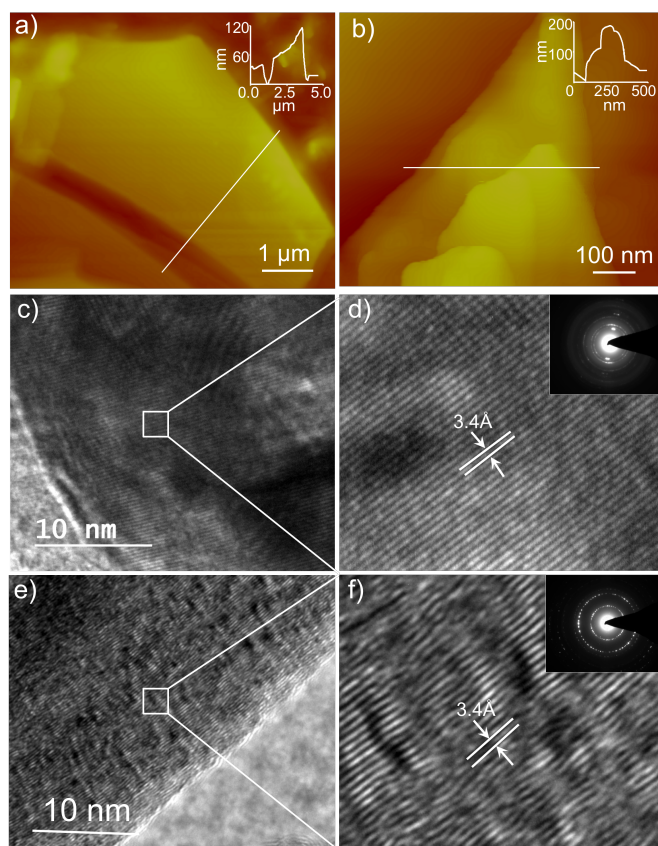
26  
27  
28  
29  
30  
31  
32  
33  
34  
35  
36  
37  
38  
39  
40  
41  
42  
43  
44  
45  
46  
47  
48  
49  
50  
51  
52  
53  
54  
55  
56  
57  
58  
59  
60

Figure 1a shows the electronic absorption spectra of **DNA1** and **DNA2**, which displays the characteristic absorptions of DNA at 260 nm ( $\epsilon_{260\text{nm}} = 1.2 \times 10^5 \text{ M}^{-1}\text{cm}^{-1}$  for **DNA1**;  $2.2 \times 10^5 \text{ M}^{-1}\text{cm}^{-1}$  for **DNA2**) and  $\pi$ -stacked HBC at 358 nm ( $\epsilon_{358\text{nm}} = 5.3 \times 10^4 \text{ M}^{-1}\text{cm}^{-1}$ ).<sup>6a</sup> Interestingly, no noticeable change is observed in the absorption spectrum of **DNA1** and **DNA2** with the increase in temperature from 20  $^{\circ}$ C to 70  $^{\circ}$ C (Figure 1a inset and Figure S2a). Dynamic light scattering (DLS) analyses of **DNA1** and **DNA2** reveal the formation of aggregates in solution with size ranging from 60 nm to 1.5  $\mu$ m and 30 nm to 1.2  $\mu$ m, respectively (Figure 1b). Furthermore, size distribution graphs for **DNA1** and **DNA2** remain unchanged even at a high temperature of 70  $^{\circ}$ C (Figure 1b inset and Figure S2b). These results imply that the strong  $\pi$ -stacking of HBC and van der Waals interaction of the alkyl chains in aqueous medium lead to the formation of thermally stable (at least stable up to 70  $^{\circ}$ C) nanostructures for **DNA1** and **DNA2**. Surface decoration of the aggregates with negatively charged DNA is evident from the zeta potential measurements of **DNA1** and **DNA2** aggregates, which show values of -15.5 mV and -17.4 mV, respectively (Figure S3). Small angle X-ray scattering (SAXS) curves of **DNA1** and **DNA2** aggregates respectively show slopes of -2 and -2.1 in the low *Q* (modulus of the scattering vector) region, confirming the formation of sheet-like nanostructures in solution (Figure 1c).<sup>9</sup> Sheet morphology of **DNA1** and **DNA2** aggregates is further established using fluorescence microscopy (Figure 1d and Figure S5), scanning electron microscopy (Figure 1e and Figure S7), and transmission



electron microscopy (TEM) analyses (Figure 1f and Figure S9). Interestingly, lateral dimensions of the sheets are several micrometers, and in some cases, extended even up to one millimeter (Figure S10), which is hard to achieve.<sup>10</sup> Sheet formation is also confirmed under different experimental conditions, demonstrating the robustness of the self-assembly (Figure S11).

Molecular level understanding of the sheet structure was obtained through atomic force microscope (AFM), high resolution-TEM (HR-TEM), and X-ray analyses. AFM height images of **DNA1** and **DNA2** display the formation of sheets on mica surface with heights of 120 nm and 200 nm, respectively (Figure 2a and b). Since the observed heights of the sheets are several folds larger than their calculated monolayer thicknesses ( $\sim$ 12 nm for **DNA1** and  $\sim$ 19 nm for **DNA2** when completely extended conformations were assumed for the molecular units), they are multilayered in nature. HR-TEM images show that the sheets consist of parallel stripes that are straight over several hundred nanometers (Figure 2c-f). These stripes can be attributed to the assembly of the amphiphiles in one dimension in a lamellar fashion with hydrophilic DNA exposed to the polar medium on either side of the supramolecular polymer chain. Furthermore, HR-TEM reveal the crystalline nature of **DNA1** and **DNA2** sheets. The distance separating the individual supramolecular polymer chain (distance between the stripes) is  $\sim$ 3.4  $\text{\AA}$  (Figure 2d and 2f). This corresponds to



**Figure 2.** AFM height images of (a) **DNA1** and (b) **DNA2** sheets and insets show the corresponding section analyses. HR-TEM images (c) & (d) of **DNA1** and (e) & (f) of **DNA2** sheets. The insets of (d) and (f) show the SAED pattern of **DNA1** and **DNA2** sheets, respectively.

the  $\pi$ - $\pi$  stacking distance of HBC core (plane-to-plane distance of  $\pi$ -stacked HBC), which permits the assembly of the individual supramolecular chain in the other dimension, leading to the formation of crystalline 2D sheets. Selected area electron diffraction patterns of **DNA1** (Figure 2d inset) and **DNA2** (Figure 2f inset) reveal bright and narrow rings, further confirm the crystalline nature of the sheets. Furthermore, a broad peak at  $2\theta = 18\text{--}33^\circ$  is observed in the wide angle XRD patterns of **DNA1** and **DNA2** sheets, which corresponds to a  $d$ -spacing of 4.9–2.7 Å, respectively (Figure S14). This can be assigned to the combination of  $\pi$ -stacking of HBC and the assembly of the alkyl chains. Based on these results, a plausible molecular model for the nanosheet is schematically depicted in Scheme 1.

It is to be noted that though the hydrophilic content of the amphiphile is increased from **DNA1** to **DNA2**, the morphology and molecular level packing of the sheets remain the same. This suggests that the self-assembly of the DNA amphiphiles is essentially dictated by hydrophobic interactions ( $\pi$ -stacking of HBC and van der Waals interaction of the alkyl chains), and the hydrophilic DNA has little influence on directing the self-assembly. It is also worth noting that no change in the sheet morphology of **DNA1** and **DNA2** is observed even

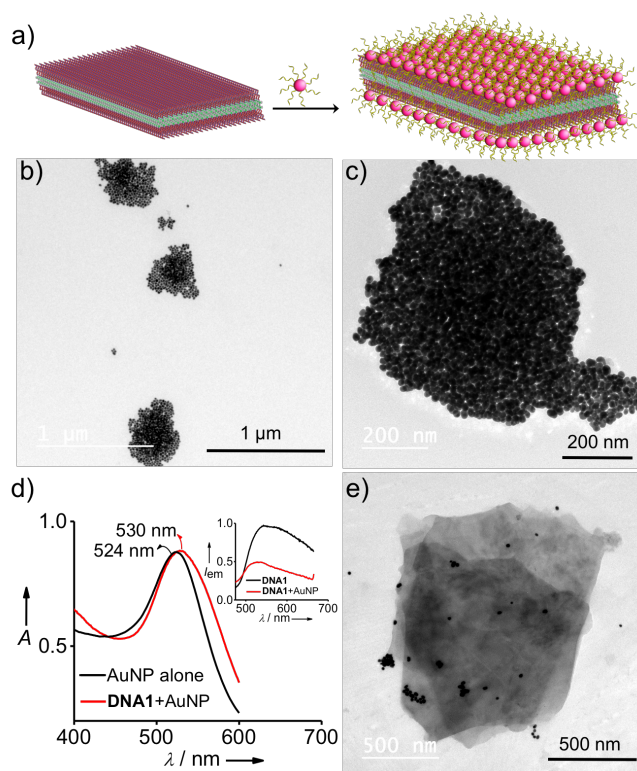


**Figure 3.** (a) Schematic representation illustrating the NP decoration on **DNA1** sheet through DNA hybridization. (b) and (c) TEM images of Au-NP decorated **DNA1** sheet. (d) Comparison of absorption spectra of Au-NPs alone and after their assembly onto **DNA1** sheet, and inset shows the corresponding emission spectral changes. (e) TEM image of a **DNA1** sheet after the self-assembly with non-complementary DNA modified NP.

after hybridization of the protruding ssDNA on the sheet surface with the corresponding complementary DNA strands (Figure S15), which is extremely important for application of the sheet as a template.

The most striking feature of the sheet is the DNA directed surface addressability, which allows the defined incorporation of other functional molecules onto the sheet surface through DNA hybridization. As a proof of concept, we demonstrate the decoration of either faces of **DNA1** sheet with  $\sim 20$  nm gold nanoparticles (Au-NPs) that are pre-modified with DNA (5'-TGGGTGCGA-3').<sup>11</sup> The DNA on the surface of the NPs is complementary to the DNA on the surface of the sheet. Self-assembly of 1:1 molar ratio of **DNA1** sheet and AuNP shows dense loading of NPs on the sheet surface (Figure 3b and 3c). It is worth noting that NPs decorates on both faces of the sheet as it is evident from the difference in contrast for the NPs present on each face. These results not only show the unique self-assembly power of DNA but also provide direct evidence for the proposed sheet structure (Scheme 1). Furthermore, interparticle surface plasmon coupling is seen due to the close packing of NPs. Accordingly, a red-shift of 6 nm is observed in the plasmon absorption band of Au-NPs that

are assembled on the sheet when compared with the corresponding non-assembled NPs (Figure 3d). Moreover, 60% quenching of fluorescence of HBC is observed (Figure 3d inset,  $\lambda_{\text{ex}} = 400 \text{ nm}$ ,  $K_{\text{sv}} = 3.7 \times 10^5 \text{ M}^{-1}$ ). Since DNA hybridization places Au-NPs at a distance of  $\sim 7 \text{ nm}$  from the HBC stacks, quenching of fluorescence can be attributed to the electronic interaction between NPs and HBC stacks.<sup>5a</sup> As expected, no decoration of NP on the sheet is observed when the self-assembly is carried out with NP modified with non-complementary DNAs (5'-TACAGCTATACTTG-3', Figure 3e) or bare NP (Figure S19), demonstrating the uniqueness of DNA-based surface addressability. Exploration of nanostructures of this kind in drug delivery (Figure S20) and catalysis are progressing in our laboratory.

In summary, we have reported for the first time, an amphiphilicity-driven self-assembly approach for the design of DNA-based surface addressable, high aspect ratio, crystalline, 2D sheets. Our results suggest that the strong self-assembling property of the hydrophobic segment of the amphiphiles essentially dictates the assembly into sheets irrespective of the chain length and rigidity of hydrophilic DNA. Hence, this approach can be applied as a general design strategy for the synthesis of DNA based micrometer-sized sheets by choosing strongly  $\pi$ -stacking moiety as the hydrophobic segment. Though nanosheets derived from the self-organization of amphiphilic systems are known in the literature, the nanosheets reported here are exceptional in many ways. The present sheet consists of a functional core (HBC-based core) and an addressable DNA shell. The dense display of highly information-rich DNA on the sheet surface offers a reversible 2D nanotemplate, which may find applications in catalysis, sensors and biomolecular recognitions. This also provides an opportunity to study DNA-mediated and distance-dependent electronic interaction between the chromophore stacks and other functional molecules of interest, and hence would be an ideal candidate for the advancement of nanoelectronics.

#### ASSOCIATED CONTENT

The Supporting Information is available free of charge on the ACS Publications website.

Experimental procedure and additional data (PDF)

#### AUTHOR INFORMATION

##### Corresponding Author

\*reji@iisertvm.ac.in

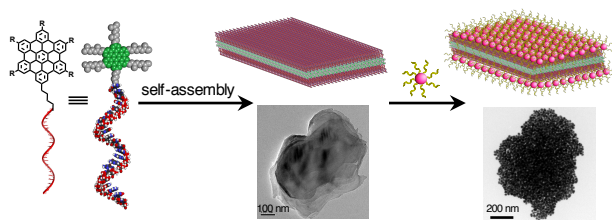
#### ACKNOWLEDGMENT

Financial supports from DBT (BT/PR7030/NNT/28/63/-2012), CSIR, and UGC are gratefully acknowledged. We thank MGU for mass analyses. We are grateful to Prof. Takuzo Aida, University of Tokyo, Japan for his suggestions on the synthesis of HBC derivatives.

#### REFERENCES

- (1) Xu, M.; Liang, T.; Shi, M.; Chen, H. *Chem. Rev.* **2013**, *113*, 3766.
- (2) (a) Chhabra, R.; Sharma, J.; Ke, Y.; Liu, Y.; Rinker, S.; Lindsay, S.; Yan, H. *J. Am. Chem. Soc.* **2007**, *129*, 10304. (b) Wilner, O. I.; Weizmann, Y.; Gill, R.; Lioubashevski, O.; Freeman, R.; Willner, I. *Nat. Nanotechnol.* **2009**, *4*, 249. (c) Voigt, N. V.; Tørring, T.; Rotaru, A.; Jacobsen, M. F.; Ravnsbæk, J. B.; Subramani, R.; Mamdouh, W.; Kjems, J.; Mokhir, A.; Besenbacher, F.; Gothelf, K. V. *Nat. Nanotechnol.* **2010**, *5*, 200. (d) Wang, D.; Zhang, G.; Zhang, Y.; Xin, L.; Dong, Y.; Liu, Y.; Liu, D. *Small* **2017**, *13*, 1700594.
- (3) (a) Seeman, N. C. *Nature* **2003**, *421*, 427. (b) Rothmund, W. K. *Nature*, **2006**, *440*, 297. (c) Aldaye, F. A.; Palmer, A. L.; Sleiman, H. F. *Science* **2008**, *321*, 1795. (d) Modi, S.; Bhatia, D.; Simmel, F. C.; Krishnan, Y. *J. Phys. Chem. Lett.* **2010**, *1*, 1994. (e) Pinheiro, A. V.; Han, D.; Shih, W. M.; Yan, H. *Nat. Nanotechnol.* **2011**, *6*, 763. (f) Jones, M. R.; Seeman, N. C.; Mirkin, C. A. *Science* **2015**, *347*, 1260901.
- (4) (a) Li, Z.; Zhang, Y.; Fullhart, P.; Mirkin, C. A. *Nano Lett.* **2004**, *4*, 1055. (b) Alemdaroglu, F. E.; Ding, K.; Berger, R.; Herrmann, A. *Angew. Chem., Int. Ed.* **2006**, *45*, 4206. (c) Thompson, M. P.; Chien, M.-P.; Ku, T.-H.; Rush, A. M.; Gianneschi, N. C. *Nano Lett.* **2010**, *10*, 2690. (d) Wu, Y.; Sefah, K.; Liu, H.; Wang, R.; Tan, W. *Proc. Natl. Acad. Sci. U. S. A.* **2010**, *107*, 5. (e) Wu, C.; Chen, T.; Han, D.; You, M.; Peng, L.; Cansiz, S.; Zhu, G.; Li, C.; Xiong, X.; Jimenez, E.; Yang, C. J.; Tan, W. *ACS Nano* **2014**, *7*, 5724. (f) Edwardson, T. G. W.; Carneiro, K. M. M.; McLaughlin, C. K.; Serpell, C. J.; Sleiman, H. F. *Nat. Chem.* **2013**, *5*, 868. (g) Zhao, Z.; Chen, C.; Dong, Y.; Yang, Z.; Fan, Q.-H.; Liu, D. *Angew. Chem., Int. Ed.* **2014**, *53*, 13468. (h) Humenik, M.; Scheibel, T. *ACS Nano* **2014**, *8*, 1342. (i) Averick, S. E.; Dey, S. K.; Grahacharya, D.; Matyjaszewski, K.; Das, S. R. *Angew. Chem., Int. Ed.* **2014**, *53*, 2739. (j) Vyborna, Y.; Vybomyi, M.; Hañer, R. *J. Am. Chem. Soc.* **2015**, *137*, 14051. (k) Kim, C.-J.; Hu, X.; Park, S.-J. *J. Am. Chem. Soc.* **2016**, *138*, 14941. (l) Banga, R. J.; Meckes, B.; Narayan, S. P.; Sprangers, A. J.; Nguyen, S. T.; Mirkin, C. A. *J. Am. Chem. Soc.* **2017**, *139*, 4278.
- (5) (a) Albert, S. K.; Thelu, H. V. P.; Golla, M.; Krishnan, N.; Chaudhary, S.; Varghese, R. *Angew. Chem., Int. Ed.* **2014**, *53*, 8352. (b) Albert, S. K.; Thelu, H. V. P.; Golla, M.; Krishnan, N.; Varghese, R. *Nanoscale* **2017**, *9*, 5425.
- (6) (a) Hill, J. P.; Jin, W.; Kosaka, A.; Fukushima, T.; Ichihara, H.; Shimomura, T.; Ito, K.; Hashizume, T.; Ishii, N.; Aida, T. *Science* **2004**, *304*, 1481. (b) Jin, W.; Fukushima, T.; Kosaka, A.; Niki, M.; Ishii, N.; Aida, T. *J. Am. Chem. Soc.* **2005**, *127*, 8284.
- (7) (a) van de Craats, A. M.; Warman, J. M.; Müllen, K.; Geerts, Y.; Brand, J. D. *Adv. Mater.* **1998**, *10*, 36. (b) Pisula, W.; Menon, A.; Stepputat, M.; Lieberwirth, I.; Kolb, U.; Tracz, A.; Siringhaus, H.; Pakula, T.; Müllen, K. *Adv. Mater.* **2005**, *17*, 684.
- (8) Tchegotareva, N.; Yin, X.; Watson, M. D.; Samori, P.; Rabe, J. P.; Müllen, K. *J. Am. Chem. Soc.* **2003**, *125*, 9734.
- (9) Yu, Z.; Tantakitti, F.; Yu, T.; Palmer, L. C.; Schatz, G. C.; Stupp, S. I. *Science* **2016**, *351*, 497.
- (10) He, Y.; Chen, Y.; Liu, H.; Ribbe, A. E.; Mao, C. *J. Am. Chem. Soc.* **2005**, *127*, 12202.
- (11) Sharma, J.; Chhabra, R.; Andersen, C. S.; Gothelf, K. V.; Yan, H.; Liu, Y. *J. Am. Chem. Soc.* **2008**, *130*, 7820.

## TOC Graphic

1  
2  
3  
4  
5  
6  
7  
8  
9  
10  
11  
12  
13  
14  
15  
16  
17  
18  
19  
20  
21  
22  
23  
24  
25  
26  
27  
28  
29  
30  
31  
32  
33  
34  
35  
36  
37  
38  
39  
40  
41  
42  
43  
44  
45  
46  
47  
48  
49  
50  
51  
52  
53  
54  
55  
56  
57  
58  
59  
60